ChemComm

Cite this: *Chem. Commun.*, 2012, **48**, 8934–8936

www.rsc.org/chemcomm

COMMUNICATION

Polypyrrole nanoparticles for high-performance *in vivo* near-infrared photothermal cancer therapy†

Mei Chen, Xiaoliang Fang, Shaoheng Tang and Nanfeng Zheng*

Received 21st June 2012, Accepted 18th July 2012
DOI: 10.1039/c2cc34463g

Polypyrrole nanoparticles (PPy NPs) exhibit strong absorption in the near infrared (NIR) region. With an excellent photothermal efficiency of ~45% at 808 nm, sub-100 nm PPy NPs are demonstrated to be a promising photothermal agent for *in vivo* cancer therapy using NIR irradiation.

Photothermal therapy, based on near infrared (NIR) laser and NIR absorbers that can convert the NIR light into heat, has been explored for cancer therapy in the past decade.[1–3] The use of NIR light is essential for photothermal therapy because of its deep penetration in tissues due to the minimal absorption of the hemoglobin and water molecules in the NIR spectral region (λ = 700–1100 nm).[4] Usually, the absorbers are delivered to the cancer cells or tumor tissues for the conversion of NIR irradiation to heat just on the morbid position without damaging normal tissues. A variety of nanomaterials acting as photothermal agents have been developed based on two factors: (1) high NIR photothermal effect and (2) good *in vivo* bio-compatibility. Many inorganic nanomaterials, such as noble metal nanostructures (*e.g.*, Au nanorods/nanoshells, and Pd nanosheets),[5–10] carbon nanomaterials (*e.g.*, carbon nanotubes and graphene),[4,11] copper chalcogenide semiconductors (*e.g.*, Cu_9S_5 and $Cu_{2-x}Se$),[12,13] have already been applied in NIR photothermal cancer therapy *in vitro* and *in vivo* in mice.

Recently, conducting polymers (*e.g.*, polyaniline, PEDOT:PSS)[14,15] have emerged as a new type of NIR photothermal therapy agent. While only *in vitro* photothermal killing of cancer cells was demonstrated for polyaniline nanoparticles, very recently highly effective *in vivo* photothermal cancer therapy by polyethylene glycol (PEG) modified PEDOT:PSS nanoparticles has been demonstrated by Liu *et al.* However, bare PEDOT:PSS nanoparticles without the modification of PEG were found to be rather toxic to cells.

We now report here our successful attempt to use sub-100 nm polypyrrole nanoparticles (PPy NPs) as a high-performance therapy agent for *in vivo* NIR photothermal cancer therapy. Without the need of any surface modification, polypyrrole is a type of highly biocompatible conducting polymer, and has been widely applied in the area of tissue engineering.[16–19] We now found that the strong absorption of PPy NPs in the NIR region can create a significant NIR photothermal effect for effective *in vivo* cancer therapy using NIR irradiation. Herein, we systematically studied the application of PPy NPs in *in vivo* photothermal cancer therapy. The strong absorption at 808 nm (2.38×10^{10} M^{-1} cm^{-1}) and high photothermal conversion efficacy (44.7%) made it a good candidate as a photothermal therapy agent. Highly efficient tumor destruction was achieved under the irradiation of 1 W cm^{-2}. By introducing SiO_2@PPy to simulate the behavior of PPy NPs, the biodistribution of PPy NPs in major organs of mice was studied. Moreover, no obvious tissue toxicity was observed for PPy NPs-injected mice.

According to a previously reported method,[20] PPy NPs were synthesized *via* aqueous dispersion polymerization using $FeCl_3$ as an oxidation agent and poly(vinylpyrrolidone) as a capping agent. Scanning electron microscope (SEM) (Fig. 1a) and transmission electron microscope (TEM) (Fig. 1b) images show that the as-synthesized PPy NPs have an average size of ~50 ± 5 nm, smaller than the average hydrodynamic diameter result (~58 nm) obtained through dynamic light scattering (DLS) (Fig. S1, ESI†). What attracted us is that the synthesized PPy NPs display strong NIR absorption with a broad peak at ~850 nm (Fig. 1c), which is characteristic of the bipolaronic metallic state of doped polypyrrole.[21] Moreover, the extinction coefficient at 808 nm was calculated to be 2.38×10^{10} M^{-1} cm^{-1}. Moreover, the as-prepared PPy NPs are highly stable in serum (Fig. S2, ESI†).

We next investigated the photothermal effect of PPy NPs. Experimentally, we examined the temperature increase of 1 mL PPy aqueous solution with various concentrations due to 10 min irradiation by the 808 nm laser with a power density of 1 W cm^{-2} (Fig. 1d). The solution containing only 20 ppm PPy NPs had an increase as high as 25 °C, while pure water had a negligible temperature change within 2 °C. Following the method developed by Roper *et al.*[22] and Hu *et al.*,[12] the photothermal conversion efficiency of PPy NPs (Fig. S3, ESI†) was calculated to be 44.7%, which is relatively high compared with those of previously reported materials.[12]

Motivated by the high NIR photothermal conversion efficiency of PPy NPs, we carried out a series of experiments to evaluate their potential as a new photothermal agent. We first

State Key Laboratory for Physical Chemistry of Solid Surfaces and Department of Chemistry, College of Chemistry and Chemical Engineering, Xiamen University, Xiamen 361005, China. E-mail: nfzheng@xmu.edu.cn; Fax: +86 592 2183047; Tel: +86 592 2186821

† Electronic supplementary information (ESI) available: Experimental details and data. See DOI: 10.1039/c2cc34463g

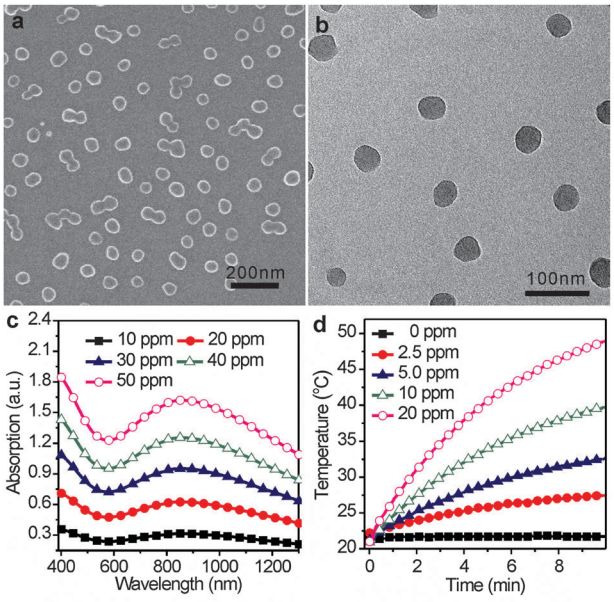

Fig. 1 Representative (a) SEM and (b) TEM images of PPy NPs. (c) UV-Vis-NIR spectra of PPy NPs at various concentrations. (d) Photothermal effect of pure water and PPy NPs with different concentrations upon the irradiation of 1 W cm^{-2} 808 nm laser.

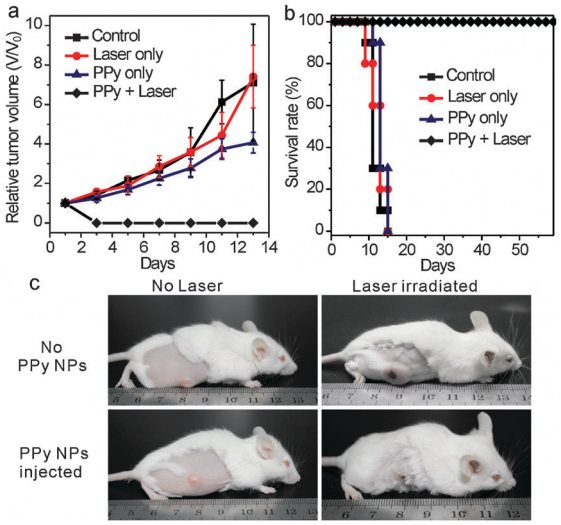

Fig. 2 *In vivo* photothermal therapy study using intravenously injected PPy NPs. (a) Tumor growth rates of groups after different treatments. (b) Survival curves of mice bearing 4T1 tumor after various treatments. (c) Representative photos of tumors on mice after various treatments (only laser treated and PPy + laser treated).

investigated the *in vitro* cytotoxicity of PPy NPs using QSG-7701 human hepatocyte cells. After incubation for 48 h with different concentrations of PPy NPs, the cell viabilities were measured by standard MTT assay. The result shows that PPy NPs have no appreciable negative effect even at a high concentration of 200 ppm (Fig. S4, ESI†).

The 4T1 tumor model on Balb/c mice was established and used to investigate *in vivo* photothermal cancer therapy application of PPy NPs. Ten mice bearing 4T1 tumor at the right rear flanks were intravenously injected with 200 μL of PPy NPs at 1 mg mL^{-1} (a dose of 10 mg kg^{-1}). After 24 h, the tumor on each mouse was exposed to the 808 nm laser with a power density of 1 W cm^{-2} for 5 min. The surface temperature of tumors on mice injected with PPy NPs reached ~60 °C after laser irradiation (Fig. S5 and S6, ESI†). Under the same irradiation conditions, in contrast, the surface temperature rise for irradiated tumors on ten uninjected mice was only ~3 °C. Another two control groups of mice with and without PPy NPs injection were not irradiated. Tumor sizes were measured every 2 days after the above treatments (Fig. 2a). All irradiated tumors on mice injected with PPy NPs disappeared 1 day after treatment, leaving the original tumor site with black scars which fell off about 1 week later (Fig. 2c). No tumor regrowth was noted in this treated group over a course of 60 days, after which the study was ended. However, tumors in other three groups showed rapid growth rates (Fig. 2a), demonstrating that only NIR laser irradiation or PPy NPs injection did not affect the tumor development. Mice in the three groups without the combined treatment of PPy NPs and NIR irradiation showed average life spans of no more than ~20 days, while mice in the combined treated group were tumor-free after treatment and survived over 60 days without any death (Fig. 2b), further demonstrating the excellent efficacy of *in vivo* photothermal cancer therapy using PPy NPs.

In order to quantitatively assess the biodistribution of PPy NPs, core–shell structured SiO_2@PPy NPs (Fig. S7, ESI†) were prepared to simulate the *in vivo* behavior of PPy NPs. In this way, inductively coupled plasma-atomic emission spectrometry (ICP-AES) can be used to analyze the accumulation of PPy NPs in each organ.[23] Compared with the radiolabeling method or fluorescent dyes labeling method, the quantification by ICP-AES is much reliable to determine the distribution of PPy NPs because there is no worry about early detaching of the labels. In this method, however, SiO_2@PPy core–shell NPs should have the similar size and surface properties to PPy NPs so that they can perfectly act the role of PPy NPs *in vivo*. As shown in the FT-IR spectra (Fig. S8, ESI†), the SiO_2@PPy NPs, that were used to substitute PPy NPs for biodistribution studies, exhibit nearly the same IR signals as PPy NPs. Moreover, the size distribution and zeta potential of SiO_2@PPy NPs (Fig. S1 and S9, ESI†) are similar to those of PPy NPs. The as-prepared SiO_2@PPy NPs were injected to Balb/c mice bearing 4T1 tumors and organs of interest (mainly heart, liver, spleen, lung, kidney and tumor) were collected after 1, 6 and 24 h. As illustrated in Fig. 3, the highest uptake of the SiO_2@PPy NPs is in liver (~56% ID g^{-1}), followed by spleen (~10% ID g^{-1}). The high accumulations of SiO_2@PPy NPs in both liver and spleen are expected since both of them are reticuloendothelial system enriched tissues. The accumulations in heart, kidney and lung are at a rather low level (<5% ID g^{-1}). In tumors, the accumulation can reach ~5% ID g^{-1}. Since there was no surface modification on the SiO_2@PPy NPs, their blood circulation half-life was only ~12 min (Fig. S10, ESI†), which might explain the relatively low accumulation of SiO_2@PPy NPs in tumors. It is expected that appropriate surface modification, for example with PEG, would enhance the accumulation of PPy NPs in tumors.[15,24]

Lastly, the potential *in vivo* toxicity of PPy NPs was investigated. No obvious sign of toxic side effects for PPy NPs injected mice at the dose of 10 mg kg^{-1} within 60 days

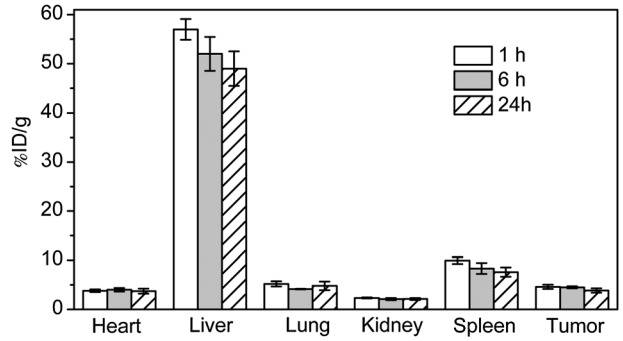

Fig. 3 Biodistribution of SiO_2@PPy in mice determined by ICP-AES of each organ. Error bars were based on three mice per group.

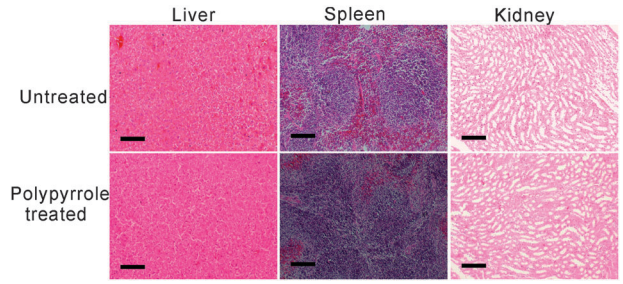

Fig. 4 Major organs H&E stained images from mice untreated and survived after photothermal therapy. Scale bar: 100 μm.

was observed. No significant body weight drop was noted in four groups (Fig. S11, ESI†). Major organs of PPy NPs treated mice, whose tumors were eliminated by the photothermal therapy, were collected 60 days after the treatment for histology analysis. No noticeable sign of organ damage was observed from haematoxylin and eosin (H&E) stained organ slices (Fig. 4 and Fig. S12, ESI†), suggesting the promise of using PPy NPs for *in vivo* photothermal cancer therapy.

In summary, we have formulated PPy NPs as a novel photothermal agent for cancer photothermal therapy. Its photothermal conversion efficiency can reach as high as 44.7% due to its strong NIR absorption. After injection with PPy NPs, tumors can be effectively ablated under the irradiation of 1 W cm^{-2} NIR laser. Both *in vitro* and *in vivo* studies indicate that the PPy NPs are highly biocompatible. An accumulation of 5% ID g^{-1} in tumors is readily achieved by PPy NPs without any surface modification. In a word, PPy NPs are an excellent candidate agent for *in vivo* NIR photothermal cancer therapy. More detailed studies on excretion, metabolism, and long-term toxicology in biological system are still underway.

This work is supported by the MOST of China (2011CB932403), the NSFC (21131005, 21021061, 20925103), the NSF of Fujian Province (Distinguished Young Investigator Grant 2009J06005) and the Fok Ying Tung Education Foundation (121011).

Notes and references

1 X. H. Huang, P. K. Jain, I. H. El-Sayed and M. A. El-Sayed, *Lasers Med. Sci.*, 2008, **23**, 217–228.
2 P. K. Jain, X. H. Huang, I. H. El-Sayed and M. A. El-Sayed, *Acc. Chem. Res.*, 2008, **41**, 1578–1586.
3 L. C. Kennedy, L. R. Bickford, N. A. Lewinski, A. J. Coughlin, Y. Hu, E. S. Day, J. L. West and R. A. Drezek, *Small*, 2011, **7**, 169–183.
4 N. W. Kam, M. O'Connell, J. A. Wisdom and H. J. Dai, *Proc. Natl. Acad. Sci. U. S. A.*, 2005, **102**, 11600–11605.
5 P. K. Jain, I. H. El-Sayed and M. A. El-Sayed, *Nano Today*, 2007, **2**, 18–29.
6 S. Lal, S. E. Clare and N. J. Halas, *Acc. Chem. Res.*, 2008, **41**, 1842–1851.
7 W. I. Choi, J. Y. Kim, C. Kang, C. C. Byeon, Y. H. Kim and G. Tae, *ACS Nano*, 2011, **5**, 1995–2003.
8 X. Q. Huang, S. H. Tang, X. L. Mu, Y. Dai, G. X. Chen, Z. Y. Zhou, F. X. Ruan, Z. L. Yang and N. F. Zheng, *Nat. Nanotechnol.*, 2011, **6**, 28–32.
9 S. H. Tang, X. Q. Huang and N. F. Zheng, *Chem. Commun.*, 2011, **47**, 3948–3950.
10 F.-Y. Cheng, C.-H. Su, P.-C. Wu and C.-S. Yeh, *Chem. Commun.*, 2010, **46**, 3167–3169.
11 K. Yang, S. Zhang, G. X. Zhang, X. M. Sun, S. T. Lee and Z. Liu, *Nano Lett.*, 2010, **10**, 3318–3323.
12 Q. Tian, F. Jiang, R. Zou, Q. Liu, Z. Chen, M. Zhu, S. Yang, J. Wang and J. Hu, *ACS Nano*, 2011, **5**, 9761–9771.
13 C. M. Hessel, V. P. Pattani, M. Rasch, M. G. Panthani, B. Koo, J. W. Tunnell and B. A. Korgel, *Nano Lett.*, 2011, **11**, 2560–2566.
14 J. Yang, J. Choi, D. Bang, E. Kim, E. K. Lim, H. Park, J. S. Suh, K. Lee, K. H. Yoo, E. K. Kim, Y. M. Huh and S. Haam, *Angew. Chem., Int. Ed.*, 2011, **50**, 441–444.
15 C. Liang, K. Yang, C. Qian and Z. Liu, *ACS Nano*, 2012, **6**, 5605–5613.
16 X. Cui, J. Wiler, M. Dzaman, R. A. Altschuler and D. C. Martin, *Biomaterials*, 2003, **24**, 777–787.
17 P. M. George, A. W. Lyckman, D. A. LaVan, A. Hegde, Y. Leung, R. Avasare, C. Testa, P. M. Alexander, R. Langer and M. Sur, *Biomaterials*, 2005, **26**, 3511–3519.
18 A. Ramanaviciene, A. Kausaite, S. Tautkus and A. Ramanavicius, *J. Pharm. Pharmacol.*, 2007, **59**, 311–315.
19 X. Wang, X. Gu, C. Yuan, S. Chen, P. Zhang, T. Zhang, J. Yao, F. Chen and G. Chen, *J. Biomed. Mater. Res.*, 2004, **68A**, 411–422.
20 H. Y. Woo, W. G. Jung, D. W. Ihm and J. Y. Kim, *Synth. Met.*, 2010, **160**, 588–591.
21 K. M. Au, Z. Lu, S. J. Matcher and S. P. Armes, *Adv. Mater.*, 2011, **23**, 5792–5795.
22 D. K. Roper, W. Ahn and M. Hoepfner, *J. Phys. Chem. C*, 2007, **111**, 3636–3641.
23 C. H. Lee, S. H. Cheng, Y. J. Wang, Y. C. Chen, N. T. Chen, J. Souris, C. T. Chen, C. Y. Mou, C. S. Yang and L. W. Lo, *Adv. Funct. Mater.*, 2009, **19**, 215–222.
24 J. Y. Chen, C. Glaus, R. Laforest, Q. Zhang, M. X. Yang, M. Gidding, M. J. Welch and Y. N. Xia, *Small*, 2010, **6**, 811–817.

